# Functionalized Nanostructures: Redox-Active Porphyrin Anchors for Supramolecular DNA Assemblies

**Karl Börjesson,[†] Joanna Wiberg,[†] Afaf H. El-Sagheer,[‡,§] Thomas Ljungdahl,[∥] Jerker Mårtensson,[†] Tom Brown,[‡] Bengt Nordén,[†] and Bo Albinsson[†,*]**

[†]Department of Chemical and Biological Engineering/Physical Chemistry, Chalmers University of Technology, S-41296 Gothenburg, Sweden, [‡]School of Chemistry, University of Southampton, Highfield, Southampton SO17 1BJ, United Kingdom, [§]Chemistry Branch, Department of Science and Mathematics, Faculty of Petroleum and Mining Engineering, Suez Canal University, Suez, Egypt, and [∥]Department of Chemistry-Medicinal Chemistry, University of Gothenburg, 41296 Gothenburg, Sweden

ARTICLE

**ABSTRACT** We have synthesized and studied a supramolecular system comprising a 39-mer DNA with porphyrin-modified thymidine nucleosides anchored to the surface of large unilamellar vesicles (liposomes). Liposome porphyrin binding characteristics, such as orientation, strength, homogeneity, and binding site size, was determined, suggesting that the porphyrin is well suited as a photophysical and redox-active lipid anchor, in comparison to the inert cholesterol anchor commonly used today. Furthermore, the binding characteristics and hybridization capabilities were studied as a function of anchor size and number of anchoring points, properties that are of importance for our future plans to use the addressability of these redox-active nodes in larger DNA-based nanoconstructs. Electron transfer from photoexcited porphyrin to a lipophilic benzoquinone residing in the lipid membrane was characterized by steady-state and time-resolved fluorescence and verified by femtosecond transient absorption.

**KEYWORDS:** DNA · nanotechnology · porphyrin · membrane · supramolecular · electron transfer

The DNA molecule has come to the fore in recent years as an excellent building block for dynamic yet robust nanotechnological applications. The highly specific hydrogen bonding in DNA provides the foundation for its programmable self-assembly properties, which have been exploited to build, mainly quite large, two- and three-dimensional supramolecular constructs.[1−4] In previous work, we demonstrated the construction of small addressable nanometer scale DNA structures based on a hexagonal unit cell, approximately 7 nm in diameter, where energy transfer can be targeted at specific locations.[5,6] Networks based on such addressability have the potential to offer spatial resolution of subnanometer precision. However, to increase the potential usefulness of dynamic DNA nanoconstructs, the transition from free diffusing to surface-attached networks is important. The lipid membrane is a surface that has been widely studied, both as flat membranes and as liposomes, and has the robustness and softness needed to anchor a dynamic nanoconstruct. Moreover, the lipid membrane is well suited to act as a bridge between the water phase and the surface onto which the lipid membrane is deposited. A common way to anchor DNA to lipid membranes is by covalently attaching a cholesterol or lipid moiety to the DNA, *via* a flexible linker (typically hexaethyleneglycol). The anchoring force is the hydrophobic affinity for the interior of the lipid membrane.

The porphyrin is a multifunctional anchor that can act as an electron and/or energy transfer component and a ligand docking site for potential coordination interactions. Furthermore, the size, shape, and hydrophobicity of porphyrins are quite similar to cholesterol, suggesting similar physical interaction for the two molecules in the lipid membrane. In recent years, several groups have used DNA as a supramolecular scaffold to control assembly of multiporphyrin systems. Porphyrins have been covalently attached to DNA on the 3′ or 5′ group of the sugar, on the phosphate backbone, on an adenine base, and as a base replacement.[7−18] Circular dichroism has been the method of choice to study these chiral porphyrin systems. To ensure that the porphyrins do not stack in the hydrophobic interior of the DNA spiral, Stulz and co-workers attached the porphyrin to the 5 position of a thymine base *via* a rigid linker.[19−21] The linker, consisting of a mono(phenylethynylene) moiety, protrudes through the major groove of the DNA helix, ensuring minimal steric interactions between the DNA and the linker.

In a previous study, we used the Stulz approach and examined a zinc porphyrin

*Address correspondence to balb@chalmers.se.

Received for review April 1, 2010 and accepted August 24, 2010.

**Published online September 1, 2010.** 10.1021/nn100667b

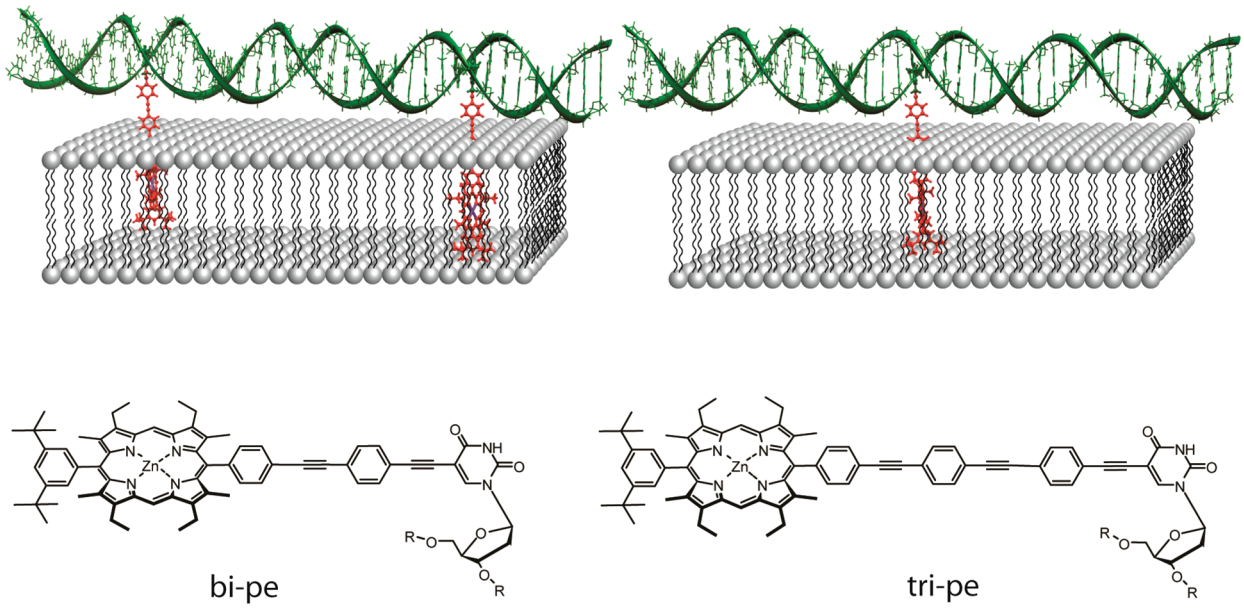


**Figure 1. Schematic picture of the supramolecular system. Top: DNA in green is covalently attached to one (right) porphyrin or two (left) porphyrin moieties (red) *via* a rigid phenylethynylene linker of variable length. The hydrophobic porphyrins are attached to a lipid membrane, forming a supramolecular system with the DNA in the water phase and the porphyrins in the lipid phase. Bottom: Porphyrins attached to a thymine base with either a bi(phenylethynylene) linker (left, bi-pe) or a tri(phenylethynylene) linker (right, tri-pe).**

covalently connected to a 14-mer DNA strand *via* a mono(phenylethynylene) linker. Owing to the hydrophobic nature of the porphyrin, it formed aggregates in aqueous solution. However, the problem of solubility was resolved by the addition of liposomes, into which the porphyrin could reside while keeping the DNA in the water phase.[22] Even though the liposomes seem to homogenize the system, certain problems remain: DNA hybridization, which gave only a 50% yield of double-stranded DNA in the free water phase, was totally obstructed when the porphyrin was anchored to the membrane. Furthermore, the fluorescence lifetime of the porphyrin in the liposome environment required two exponentials with about 50% weight each to explain the fluorescence decay. Even though these results suggested a quite heterogeneous system, it was still sufficiently homogeneous to show sequential energy and electron transfer. Energy transfer was obtained from a fluorescein covalently attached to the complementary DNA strand in the water phase, to the linked porphyrin. The porphyrin, now in its excited state, was subsequently oxidized by a benzoquinone molecule in the lipid membrane.[22] The study demonstrated the usefulness of a multifunctional lipid membrane anchor that can work not only as an anchor but also as an energy donor/acceptor, a redox center, a coordination site, and a structural probe.

In the present study, we wish to address the anchoring of the porphyrin to the liposome and the hybridization of the DNA anchored to the membrane by using one or two porphyrins (Figure 1). To facilitate the hybridization, two improvements have been made. First, the DNA length has been increased from 14 base pairs to 39 base pairs, which should increase the driving force of duplex formation. Second, the porphyrin−DNA linker has been extended; two new lengths of linkers have been synthesized, with 2 or 3 repetitive phenylethynylene moieties. The addition of each of these moieties results in approximately 7 Å increase in linker length and, thus, DNA−liposome separation, resulting in reduced liposome−DNA repulsion and increased space for the DNA hybridization event. In this study, we determine the binding characteristics of the novel porphyrin−DNA complex to a lipid membrane and furthermore explore the DNA hybridization pathway on the liposome surface. Finally, the functionality of the porphyrin anchor is demonstrated by probing electron transfer reactions from the photoexcited zinc porphyrin to a lipophilic benzoquinone residing in the interior of the membrane.

## RESULTS AND DISCUSSION

**Synthesis.** The porphyrin-containing oligonucleotides were synthesized using protected and activated nucleotides **3a** and **b** (Scheme 1) using standard solid phase phosphoramidite oligonucleotide synthesis techniques. The porphyrin nucleotides were constructed by first attaching the phenylethynylene linker to the DMT-protected uridine nucleoside using standard Sonogashira reaction conditions followed by attaching the free-base porphyrin using copper-free Sonagashira reaction conditions.[23] The reason for using copper-free conditions in the last step was to avoid copper incorporation into the porphyrin. The building block method used here demonstrates a convenient way of producing porphyrin-tagged DNA, with different linker molecules, in high yield.

The oligonucleotides were synthesized using the free-base porphyrins and also postmodified with $Zn(OAc)_2$ in methanol to produce the zinc porphyrins. The reason for the postsynthetic metalation is to avoid the acidic conditions on the solid phase synthesizer, which would otherwise have caused demetalation. Interestingly, it has been noticed that zinc insertion is also facile at 40 °C using a few equivalents of $ZnCl_2$ in buffered (pH = 8) solution. For reaction conditions, see Supporting Information.

**Porphyrins on DNA.** The hydrophobic porphyrin together with the hydrophilic DNA creates an amphiphilic molecule. How well the molecule is solvated in water is not easily predicted, but in contrast to commonly used membrane anchors (cholesterol/lipid), the change in spectral properties of the porphyrins can be used to probe possible aggregation. As can be seen in the CD spectra for the porphyrin−DNA adduct (Figure 2), only the DNA gives any substantial signal (between 200 and 300 nm). In contrast to our previous study (using a 14-mer oligonucleotide and a mono(phenylethynylene) porphyrin−DNA linker), where the porphyrin gave rise to a relatively strong bisignate CD signal at ~415 nm, the zinc porphyrins now (using a 39-mer oligonucleotide) only show a small negative CD signal (at ~415 nm). A weak, single-sign CD band with the same shape as the absorption is most likely a so-called "induced CD" from the chiral environment of DNA, whereas a stronger bisignate CD feature could indicate a porphyrin dimer, in which the porphyrins are chirally arranged relative to each other, or the formation of larger aggregates. Differences in length between the linkers that were used in the two studies cannot explain this result since a longer linker would decrease the electrostatic repulsion of the DNA for two interacting porphyrins on separate DNA strands. Consequently, it is the longer DNA strand that enhances the solubility of the porphyrins. However, a 39-mer oligonucleotide with two zinc porphyrin anchors is observed to aggregate in water solution (seen as broadening of the absorption spectra). Therefore, it is not the length of the DNA that alone determines if the porphyrins will aggregate in water solution, but it is the ratio of the number of porphyrins to DNA bases that is the decisive factor.

**Membrane Anchoring.** To determine if the porphyrin−DNA complex can anchor to a liposome, flow linear dichroism was used. In flow linear dichroism, a shear flow is used to orient large molecules with a defined long axis.[24] The porphyrin-tagged oligonucleotide is too small to be oriented by itself, but the large soft liposome becomes distorted into an ellipsoidal shape from the shear gradient, with the long axis oriented in the flow direction, and thus all molecules bound to the liposome in a nonrandom manner also become oriented. There are three distinct peaks in the $LD^r$ spectra in Figure 3, one at 350 nm, one at 415 nm, and one at 550 nm. The sheer presence of a signal

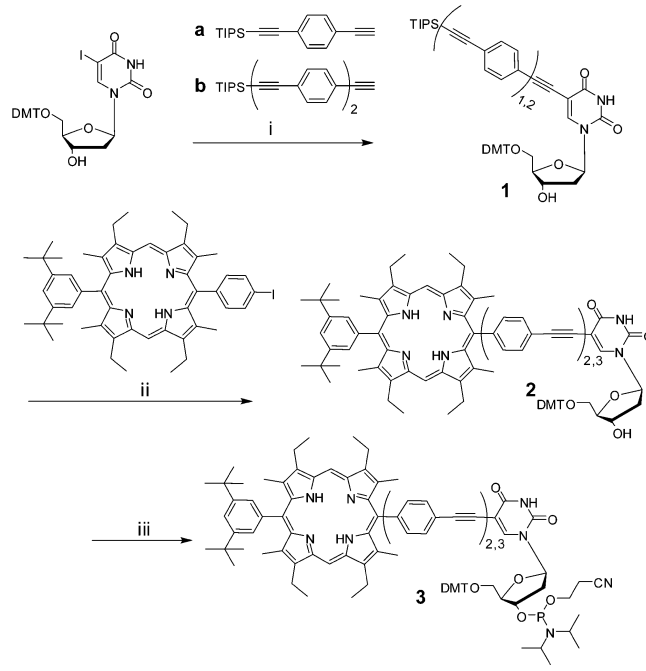


**Scheme 1. Synthesis of the porphyrin nucleoside building block 3a (bi(phenylethynylene) linker) and 3b (tri(phenylethynylene) linker). Conditions: (i) $Pd_2(dba)_3$, CuI, $AsPh_3$, $NEt_3$, 1a 69% and 1b 90%; (ii) (a) TBAF, THF, (b) $Pd_2(dba)_3$, $AsPh_3$, DABCO, DMF/THF, 2a 86% and 2b 69%; (iii) $N(iPr)_2P(Cl)O(CH_2)_2CN$, DIPEA, $CH_2Cl_2$, 3a 72% and 3b 63%.**

proves that the porphyrins are anchored into the liposome in a defined way. Additionally, the signal strengths are comparable with molecules known to orient well in lipid membranes,[25,26] thus suggesting that the porphyrin nucleosides also are well oriented. Furthermore, the negative sign of the signals indicates that the transition dipole moments responsible for each signal are located with an average angle of less than 55° with respect to the liposome normal.

The porphyrin anchor with its oligo(phenylethynylene) linker is a composite chromophore. The linker and the porphyrin moieties are only weakly coupled

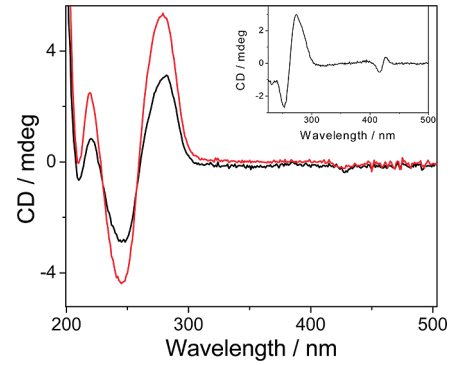


**Figure 2. CD spectra of double-stranded porphyrin−DNA adducts in solution (absence of liposomes) for bi(phenylethynylene) linker (red) and tri(phenylethynylene) linker (black). Also shown (from ref 22) as an inset is the spectrum for a mono(phenylethynylene) linker. CD at 200−300 is mainly due to DNA itself. With bi-pe and tri-pe, only weak induced CD is seen at the Soret 415 nm absorption band, while with mono-pe (inset), the bisignate exciton CD feature indicates chiral porphyrin aggregates.**

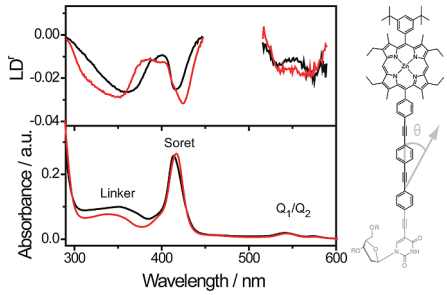


**Figure 3. Linear dichroism (LD) spectra of double-stranded porphyrin−DNA adducts anchored to membrane of flow-aligned liposomes. Absorbance (bottom) and normalized "reduced" linear dichroism $LD^r = LD/A$ (top) for the cases of bi-pe (red) and tri-pe (black) linkers between porphyrin and DNA. To the right, tri-pe is depicted together with the definition of transition moment directions.**

electronically, and this leads to well-defined regions in the spectrum that could be ascribed to these two parts. The porphyrin has absorption bands at 415 nm, the so-called Soret band, and a pair of peaks at 540 and 570 nm denoted Q-bands. The linker absorbs close to 350 nm, somewhat depending on the conjugation length. In order to assist the assignment of the polarized-light spectroscopy results, a quantum mechanical calculation on the tri-pe chromophore (see Figure 3) was made. Calculated energies, oscillator strengths, and electric transition dipole moment directions for the first five singlet electronic transitions are presented in Table 1, together with assignments of transitions in the experimental spectrum. The four lowest electronic transitions are assigned to the porphyrin moiety and resemble the corresponding transitions observed for an isolated zinc porphyrin.[27,28] In a high symmetry ($D_{4h}$) porphyrin, both the Q- and Soret bands are due to degenerate transitions uniformly polarized in the molecular plane. When the porphyrin is substituted, the symmetry is lowered and the degeneracy is broken. This does not generally lead to a visible splitting of the absorption components but may have a dramatic effect on the transition moment directions. For the specific chromophore used in this study, the substitution leads to a pair of overlapping Q-bands with almost perpendicular transition moments polarized close to 45° to the molecular long axis. For the Soret band, the symmetry lowering instead leads to a pair of perpendicular transitions polarized either along or perpendicular to the long axis. Finally, the linker part of the anchor has, as expected, a lowest singlet energy transition ($S_0 \rightarrow S_5$) that is long-axis-polarized.

**TABLE 1. Calculated Electronic Transition Parameters for tri-pe Chromophore: Wavelength (λ), Oscillator Strength (*f*), and Transition Moment Direction (θ Relative to Molecular Long Axis in Figure 3) According to an INDO/S Calculation on an AM1 Optimized Ground-State Structure: Assignment of Experimental Spectral Features**

| transition | assignment (observed peak) | λ/nm | *f* | θ/deg |
|---|---|---|---|---|
| $S_0 \rightarrow S_1$ | $Q_1$ (542,573 nm) | 610 | 0.05 | 48 |
| $S_0 \rightarrow S_2$ | $Q_2$ (542,573 nm) | 597 | 0.12 | −20 |
| $S_0 \rightarrow S_3$ | $Soret_1$ (415 nm) | 351 | 5.3 | 3 |
| $S_0 \rightarrow S_4$ | $Soret_2$ (415 nm) | 347 | 2.9 | −84 |
| $S_0 \rightarrow S_5$ | linker (350 nm) | 310 | 0.21 | 0 |

With these assignments, the observed polarized absorption spectrum could be fully explained. In the linker region of the spectrum (around 350 nm), both anchors show a strongly negative $LD^r$ in accordance with the long axis polarization of this transition. In the Soret region (400−450 nm), the polarization goes from close to zero to a negative value of similar magnitude as the linker transition, in perfect agreement with the predicted polarization pattern. Finally, for the Q-bands, the $LD^r$ values are intermediate, indicating a more oblique angle of the corresponding transition moments.

To further characterize the porphyrin membrane anchoring, the porphyrin lipid binding constants were determined for the two different linker lengths (for binding isotherms, see Supporting Information). This was done by monitoring the absorbance change of the Soret band (at 415 nm) or the emission change (at 635 nm) with respect to lipid concentration. The binding site should contain more than one lipid molecule, and if the binding site size, *n* (binding sites/lipids), is introduced, the standard equilibrium equation can be expressed as

$$K = \frac{[P_{Lip}]}{[P_{Water}][\text{free binding sites}]} = \frac{[P_{Lip}]}{[P_{Water}]([L_0]n - [P_{Lip}])}$$

where $[P_{Lip}]$ is the concentration of porphyrins bound to the liposome, $[P_{Water}]$ is the concentration of porphyrins in the water phase, and $[L_0]$ is the lipid concentration. The equilibrium equation can be rearranged to express the total amount of liposome-bound porphyrin:

$$[P_{Lip}] = \frac{\left(\frac{1}{K} + [P_{tot}] + n[L_0]\right)}{2} - \sqrt{\frac{\left(\frac{1}{K} + [P_{tot}] + n[L_0]\right)^2}{4} - [L_0][P_{tot}]n}$$

where $[P_{tot}]$ is the total porphyrin concentration. In the analysis, the binding was assumed to go to completion at high lipid concentration, and at intermediate lipid concentrations, the spectra were treated as a linear combination of the unbound and bound states. Using the equation above, the binding constants were calculated as $2.6 \times 10^6$ and $8.6 \times 10^6\ M^{-1}$ for bi-pe and tri-pe, respectively, and the binding site size was determined to be 0.21 and 0.25 sites/lipid for bi-pe and tri-pe, respectively. The size of the binding site is about what could have been expected for a free porphyrin but is smaller than expected, taking the relatively large size of the DNA molecule in the water phase into account.

It is very interesting to compare the binding site strength and size for DNA anchored to liposomes by

one or two anchors. At room temperature, the doubly porphyrin modified strands are aggregated, which results in very slow binding to lipid membranes, and therefore, the binding isotherms for these strands are measured at 40 °C. The binding strengths for the doubly anchored DNA were determined to be $2 \times 10^7$ $M^{-1}$ for both bi-pe and tri-pe (for comparison, the binding strength for DNA anchored with a single tri-pe was determined to be $3 \times 10^6$ $M^{-1}$ at 40 °C), and the binding site sizes were determined to be 0.013 and 0.017 sites/lipid for bi-pe and tri-pe, respectively. In comparison to DNA attached by a single anchor, the doubly anchored DNA covers about a factor 15 larger surface area, and furthermore, the larger area is of about the same size as the predicted area of a 39-mer double-stranded DNA (see Supporting Information for derivation). Consequently, two anchor points are necessary to force double-stranded DNA in a tangential position to the membrane surface, and if only one anchor point is used, the strong anchoring of the porphyrin must force the DNA to bend in a V shape to fit, in accordance to the small binding site. The binding strength was increased by 1 order of magnitude going from one anchor to two, deviating substantially from the square dependence on binding strength expected. Supposedly, this deviation is mainly due to the force needed to position the whole DNA strand close to the membrane surface.

It is interesting to compare the liposome binding strength of the porphyrins with other DNA-tagged liposome binding molecules, such as cholesterol. The binding constant between a cholesterol-tagged single-stranded DNA oligonucleotide and a flat double layer lipid membrane has been estimated using a quartz crystal microbalance to be $6 \times 10^7$ $M^{-1}$.[29] The difference between the binding constants for the porphyrin- and cholesterol-tagged DNA is quite large, at least for bi-pe. However, it should be noted that the porphyrin carries double-stranded DNA where the porphyrin is less embedded into the liposome than in the single-stranded case (*vide infra*). Furthermore, the cholesterol is an end modification with a flexible linker to the DNA, allowing the DNA to be well separated from the lipid membrane, in contrast to the porphyrin that ought to force the DNA to adopt a more tangential orientation to the liposome surface.

The two different porphyrin anchors have liposome binding constants that differ by approximately a factor of 3. The reason for this might be that the DNA liposome distance, and thus repulsion, is less for tri-pe or that tri-pe gives the porphyrin space to become more embedded in the hydrophobic interior of the liposome. The more embedded porphyrin might have a stronger anchoring ability, or the fact that a part of the hydrophobic linker also is embedded in the membrane will add to the binding strength. Figure 4 shows the emission spectra for the porphyrin−DNA adducts in water and liposome environment. The emission maxima are

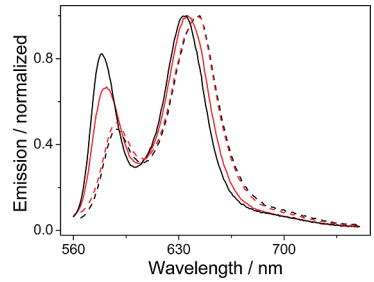


**Figure 4. Emission of porphyrin−DNA adducts (red, bi-pe; black, tri-pe) in buffer solution (dotted line) and in liposomes (straight line). The different ratio between the two vibronic emission peaks is due to different accessibility to water acting as a weakly coordinating Lewis base.**

shifted a few nanometers for the two different environments, but more importantly, the ratio between the two emission peaks is changed. Moreover, the change is larger for tri-pe than for bi-pe. It has been shown, for zinc porphyrins with the same substitution pattern, that the emission peak ratio is sensitive to the accessibility of Lewis bases; coordination of a Lewis base leads to a decreased ratio of the 580 and 630 nm emission peaks.[30] Here water acts as a weak Lewis base, and consequently, the porphyrin attached with tri-pe should be more embedded in the lipid membrane than the one attached with bi-pe (*i.e.*, less accessible to water). This ought to be the reason for the higher binding strength for tri-pe.

To further investigate the binding depths of the porphyrin−DNA adducts, three kinds of modified lipids, having carbonyl groups on different membrane depth, were used (Figure 5). The carbonyl oxygen coordinates to the zinc atom in the porphyrin *via* its lone pair, resulting in a decrease in the ratio between the intensities of the two emission peaks. Targeting the depth information using coordination to the zinc atom has two advantages over a more standard fluorescence quenching approach.[31] First, the sensitivity of the measurement is increased using an internal reference (ratio of the emission peaks) rather than an external reference (changes in emission between samples). Second, the spatial resolution is increased using the small zinc atom as a target, as compared to using the large porphyrin fluorophore as a target. In Figure 5, the emission ratio for the porphyrin−DNA with respect to lipid modification site is shown. The data are arranged with the unmodified lipid to the left and the lipids with additional carbonyl modifications at increasing membrane depths to the right. If the inserted zinc porphyrin can coordinate with the carbonyl group on the lipid, a decrease in the ratio between the intensities of its emission peaks (580 nm/630 nm) is expected. For double- and single-stranded tri-pe and for single-stranded bi-pe, the data for the binding depth have minima for the two modified lipids with carbonyls positioned at intermediate depths. This indicates that the position of the zinc atom for these constructs is close to the middle of

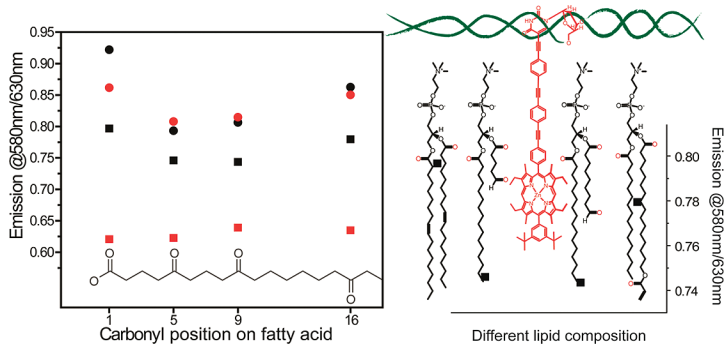


**Figure 5. Left: Emission ratio (580 nm/630 nm) as a function of modification site of the lipids (10 mol% modified lipids in DOPC) for single-stranded (circles) and double-stranded (squares) porphyrin−DNA complexes (tri-pe black, bi-pe red). Right: Enlargement of data set for double-stranded tri-pe and interpretation of the binding depth with the help of the positions of the carbonyl groups.**

the outer leaflet of the membrane. For the double-stranded bi-pe case, the peak ratio is comparably small for all four lipids and no variation with position of the additional carbonyl group can be seen. This suggests that the zinc atom on average is close to the regular ester carbonyl groups of the lipids and close to the surface of the membrane. Consequently, the double-stranded bi-pe adduct is not as deeply inserted into the membrane as the corresponding single-stranded adduct. This result furthermore shows that the double-stranded tri-pe complex penetrates deeper into the membrane than the shorter bi-pe as expected from simple modeling. An estimated location of the tri-pe adduct in the membrane is depicted in the right panel of Figure 5.

**DNA Hybridization on the Membrane.** It has been shown that a 14-mer DNA strand connected to a porphyrin *via* a mono-pe linker cannot hybridize with a complementary strand in the presence of liposomes.[22] It is believed that the porphyrin pulls the DNA so close to the liposome surface that the hybridization is sterically prohibited. Therefore, by increasing the length of the linker, and thus, increasing the DNA−membrane distance, the hybridization should be more facile. Undoubtedly, the UV melting curves in Figure 6 show that hybridization indeed can occur at the membrane surface and can do so both for a porphyrin−DNA strand hybridizing with an unmodified strand as well as for two DNA strands that both carry porphyrin anchors. Moreover, the melting temperature of the porphyrin−DNA connected through the tri-pe linker is increased in the presence of liposomes. The increase in melting temperature is small when a porphyrin strand is hybridized with an unmodified complementary strand. However, when the complementary strand also carries a porphyrin, the melting point increase is significantly larger. This is probably due to the fact that both strands are attached to the membrane, and thus, the effective concentration is increased or that the liposome removes the porphyrin from unwanted interactions during the hybridization. It should be noted that, even though the melting temperature is higher in presence of liposomes, it is still lower than for the unmodified DNA ($T_m$ = 81 °C), indicating that the porphyrin lowers the stability of the DNA duplex. In order to compare the influence from the linker length, the two 39-mer constructs with the bi-pe and tri-pe linker were studied. The porphyrin connected with the bi-pe linker in contrast to the longer linker does not seem to give an increased melting temperature in the presence of liposomes, thus showing the importance of the linker length when hybridizing DNA on a membrane surface. These results show that the porphyrin−DNA complex can hybridize on a membrane surface and that, for tri-pe, the melting temperature is slightly increased when anchored to the lipid membrane.

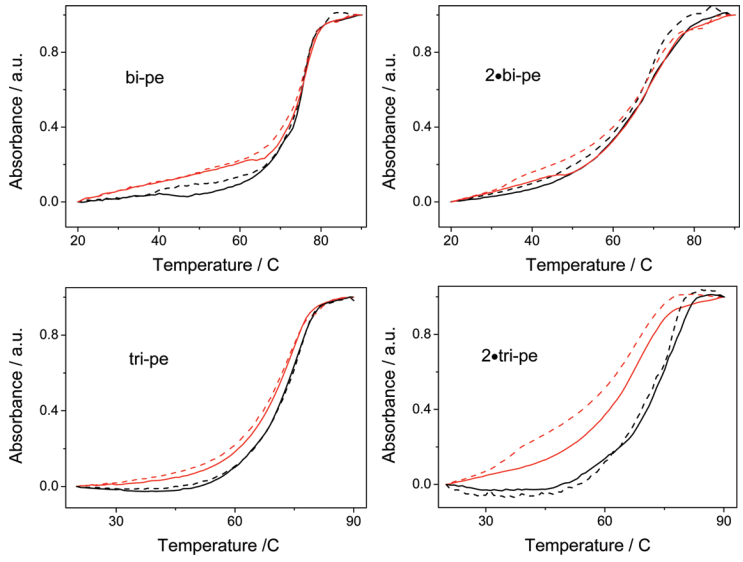


**Figure 6. UV melting curves (absorbance at 260 nm) in the absence (red) and in the presence (black) of liposomes; solid and dashed lines represent increase and decrease of temperature, respectively. Top and bottom rows show melting curves using bi-pe and tri-pe, respectively. Left and right columns show melting curves with one or two (on separate strands) porphyrin modifications, respectively.**

From the melting curves, it cannot be ruled out that the difference in melting temperature between the linkers is due to the different binding constants to the liposome. In fact, the porphyrin is probably quite mobile and able to transiently withdraw more or less completely from the membrane, more frequently at elevated temperatures. Two extreme models of DNA hybridization are shown in Figure 7: either the hybridization occurs close to the liposome surface or in bulk solution; in the latter case, a smaller or larger fraction of unbound porphyrin−DNA adduct (larger at elevated temperature) may be envisaged.

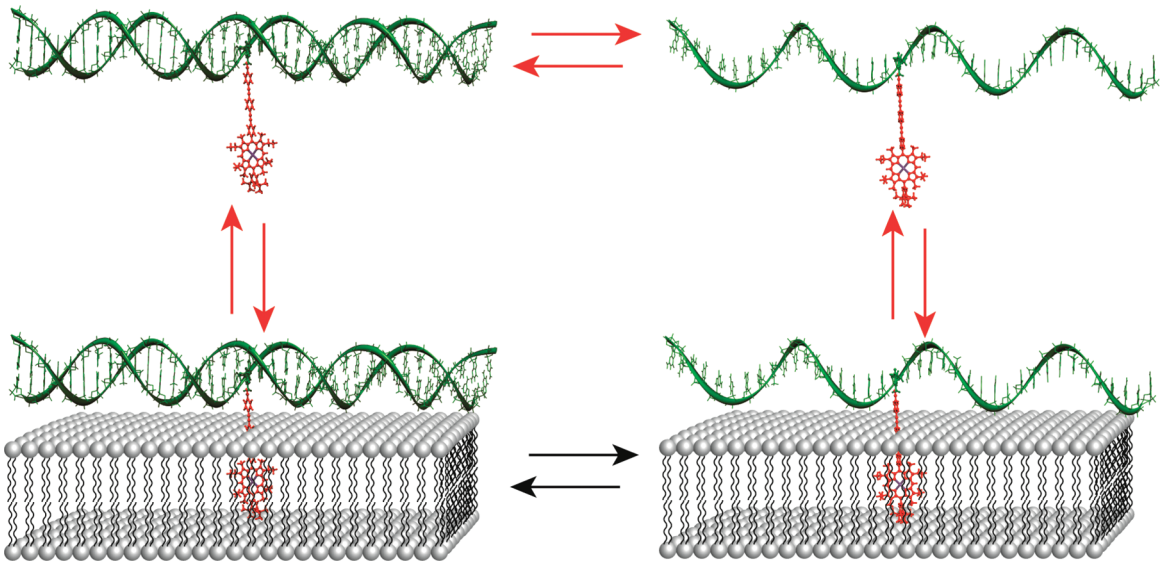

**Figure 7. Simplified extreme models for DNA hybridization at lipid surface. Hybridization occurs either on the liposome surface (black arrows) or in bulk water phase (red arrows). See text for explanation.**

To examine if the amount of porphyrin bound to liposomes changes significantly at elevated temperatures, the emission spectra for porphyrins bound to liposomes were measured at several temperatures (Figure 8). The ratio between the two emission peaks of the zinc porphyrin was not decreased when increasing the temperature, but instead, it was raised in a sigmoidal shape similar to the 260 nm absorbance melting curve. That the emission peak ratio is increased when increasing the temperature suggests that the single-stranded porphyrin is more deeply anchored into the membrane and less accessible to water, which is in perfect agreement with the measured binding depths (*vide supra*). Moreover, the binding strength is enhanced for the single strand ($1.4 \times 10^7$ $M^{-1}$, bi-pe at 40 °C) as compared to the double strand ($2.6 \times 10^6$ $M^{-1}$, bi-pe at room temperature). This is expected because, as the conformational flexibility is greater, the bases are hydrophobic and the load is less for the single-stranded complex. As a result, the hybridization seems to occur with the DNA molecules attached to the liposome surface; that is, the pathway indicated with black arrows in Figure 7 is the more likely one, both for the dissociation and hybridization step.

**Electron Transfer and System Homogeneity.** To illustrate the potential of a porphyrin, as compared to inert cholesterol, as a membrane anchor, electron transfer between the zinc porphyrin donor and the membrane residing 2,6-di-*tert*-butyl-*p*-benzoquinone acceptor is demonstrated (see Supporting Information). Electron transfer between zinc porphyrins and benzoquinone in the presence of liposomes has been shown to be very efficient, and we therefore wanted to use this pair to probe charge transfer in the more static DNA−porphyrin constructs.[32] The amount of electron transfer for the porphyrin−DNA adducts connected with bi-pe and tri-pe was monitored as quenching of porphyrin fluorescence or reduction of fluorescence lifetime as a function of benzoquinone concentration (see Supporting Information). Similar to our previous study on porphyrin−DNA, connected through a mono-pe linker and subjected to fluorescence quenching by benzoquinone in liposomes, both a dynamic and a static Stern−Volmer quenching component, with approximately the same magnitudes for the three different linker lengths, can be observed.[22] The dynamic quenching was determined using time-resolved single photon counting, where the fluorescence decay of the

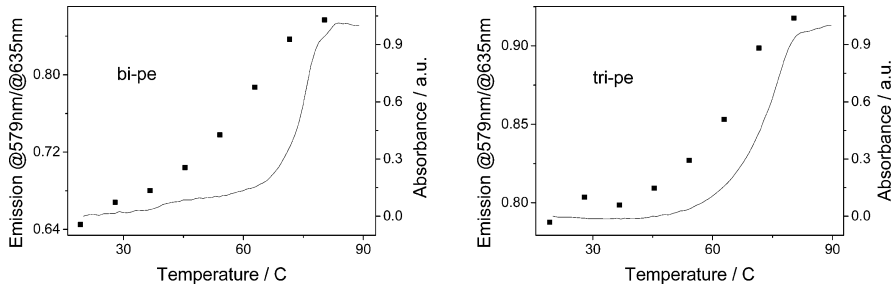


**Figure 8. Emission ratio (Em579/Em635 nm, squares) of porphyrin−DNA complexes as a function of temperature (left, bi-pe; right, tri-pe). DNA absorbance (at 260 nm) melting curve is inserted for comparison (solid line).**

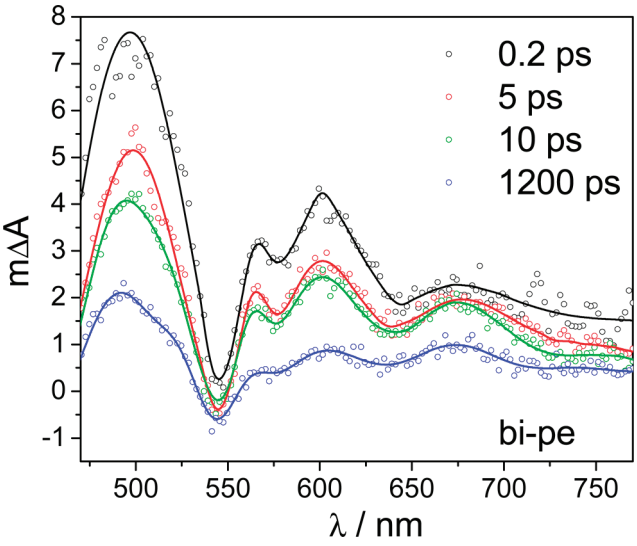


**Figure 9. Transient absorption spectra of bi-pe in liposome environment at delay times noted. The excitation wavelength was 420 nm. The signature of the ZnP radical cation at 680 nm is clearly seen already after 200 fs and lingers through the studied 1200 ps interval. The differential absorbance is normalized to a ground-state absorbance of 1 at the excitation wavelength.**

unquenched porphyrin needed two exponentials ($\tau_1$ = 1.5 ns and $\tau_2$ = 0.2 ns) to fit the data. For all of the oligo-pe linkers, when the porphyrin−DNA adducts and liposomes were mixed at room temperature, the preexponential weights for the two decay components were about 50% each, indicating a very heterogeneous system. Ideally, only one decay component should be needed to explain the fluorescence decay for the porphyrin−DNA complexes anchored to the liposome, and the fluorescence lifetime for an unquenched zinc porphyrin is about 1.5 ns. Furthermore, only the 1.5 ns lifetime was seen to be subjected to benzoquinone quenching. However, the preexponential factor for the long lifetime could be raised to 85% by gentle heating and cooling of the samples, thus resulting in a more homogeneous system. This suggests that the short lifetime comes from a kinetically trapped species and, moreover, that the system is sensitive to the formation procedures.

Now we wish to detect the porphyrin radical cation to prove that the fluorescence quenching indeed is electron transfer. Thus femtosecond transient absorption was measured for both bi-pe and tri-pe in the presence of benzoquinone in the liposomes corresponding to approximately 50% steady-state emission quenching. Due to the low optical density in the Q-band, the porphyrins were instead excited in the Soret band, thus giving a $S_0 \rightarrow S_3/S_4$ transition from where internal conversion to $S_1$ occurs within a few picoseconds or faster. The ZnP radical cation is known to absorb at around 680 nm,[33−35] and as is shown in Figure 9, the spectral signature of radical formation is present already after 0.2 ps. Comparing spectra normalized to the ground-state absorption at the excitation wavelength for the quenched and unquenched systems at this time delay gives indications of the static quenching. By comparing the peak heights at the $S_1 \rightarrow S_n$ absorption maximum (at ~490 nm), around 30% static quenching is observed for both linkers, which is in agreement with the estimations made from the steady-state fluorescence. The peak at 680 nm is still present after 1200 ps, which indicates formation of long-lived charge-separated states within the porphyrin−DNA liposome system. Longevity of the radical states is crucial for future applications in, for example, molecular scale electronics. After 1200 ps, the total quenching includes also the dynamic component and is estimated to be approximately 50% for both bi-pe and tri-pe by the comparison of signal strength from the ZnP triplet, which also absorbs in the 490 nm region. This agrees well with the amount of steady-state quenching at the concentrations of benzoquinone employed.

The decay traces at 680 nm for both bi-pe and tri-pe in the presence of benzoquinone as well as the unquenched tri-pe system are shown in Figure 10. The differences between the quenched and unquenched system are clear and most evident at ultrashort delay times. The fast initial decay, probably due to the $S_{3/4} \rightarrow S_1$ internal conversion, observed for the reference system is absent and replaced by a buildup in the same time scale when benzoquinone is present. This could indicate ultrafast electron transfer from the higher excited state and is related to the static quenching of the system. A quantitative estimation of the rate constants for the static and dynamic components of the electron transfer was not attempted due to the complexity of the decay traces.

## CONCLUSION

In conclusion, we have characterized each step in the assembly of the supramolecular system shown in

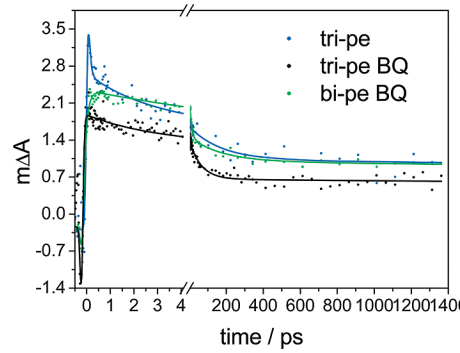


**Figure 10. Transient absorption traces at 680 nm of bi-pe and tri-pe in a liposome environment with benzoquinone present, corresponding to 50% steady-state emission quenching, as well as the trace from the tri-pe reference with no benzoquinone present. The differential absorbance is normalized to a ground-state absorbance of 1 at the excitation wavelength 420 nm. For the unquenched system, a fast initial relaxation is seen, which is absent for the samples with benzoquinone present. This indicates ultrafast static electron transfer from the porphyrin to the benzoquinone.**

Figure 1. This construct will be used in DNA-based nanotechnology where the unprecedented spatial resolution of redox centers (the porphyrins) is envisioned to be important in many potential applications ranging from artificial photosynthesis to novel lithographic techniques (on supported lipid bilayers). In this respect, when the nanoassembly becomes large, a sturdy DNA building block with optimized lipid binding properties and predictable hybridization performance is of the utmost importance. For example, the fact that at least two anchors are necessary for achieving a flat network on a lipid surface is an important result from this study. Furthermore, the key building block in the supramolecular system, the porphyrin thymidine nucleoside, was optimized with respect to the porphyrin−DNA linker moiety. The nucleoside is synthesized using a building block procedure that ensures high yield and ease of linker modifications. Liposome porphyrin binding characteristics, such as orientation, strength, homogeneity, and binding site size, are determined, suggesting that the porphyrin is well suited as a photophysical and redox-active lipid anchor, in comparison to the inert cholesterol anchor commonly used today. The binding studies show that two anchors are needed to force the DNA to a tangential position on the lipid surface. Moreover, the hybridization properties of the liposome-bound double-stranded DNA indicate that the liposome can stabilize the DNA structure for the porphyrin-tagged oligonucleotides provided that the porphyrin−DNA linker is sufficiently long, presumably by removing the hydrophobic porphyrin from the vicinity of the DNA and by increasing the local DNA concentration on the lipid surface. To demonstrate the usefulness of an active lipid binder, electron transfer between the excited-state porphyrin and a benzoquinone electron acceptor is verified. Finally, this porphyrin functional unit will become important when a DNA membrane anchor combined with an active center is required and, furthermore, when the membrane anchoring needs to be spectroscopically probed.

## EXPERIMENTAL SECTION

**Liposome Preparation.** 1,2-Dioleoyl-*sn*-glycero-3-phosphocholine (DOPC) was purchased from Larodan. Carbonyl-modified lipids (1-palmitoyl-2-(5′-oxovaleroyl)-*sn*-glycero-3-phosphocholine, 1-palmitoyl-2-(9′-oxononanoyl)-*sn*-glycero-3-phosphocholine, and 1-palmitoyl-2-[16-(acryloyloxy)palmitoyl]-*sn*-glycero-3-phosphorylcholine) were purchased from Avanti and used at 10 mol % together with DOPC. Large unilamellar vesicles (LUVs) were prepared by standard procedure as briefly described here. A thin lipid film was created by evaporating a chloroform solution of the lipids, which was subsequently dissolved in aqueous buffer and subjected to freeze−thaw cycling (5 times). The solution was then extruded 21 times through 100 nm polycarbonate filters (Whatman). Dynamic light scattering (DLS) was used to confirm the size (radius ∼50 nm) and monodispersity (polydispersity index <0.1) of the liposomes. DLS was performed on a Malvern Zetasizer Nano zs at a lipid concentration of 20 μM.

**Photophysical Measurements.** All measurements were made in a Tris-HCl buffer at pH 8 in total sodium ion and Tris concentrations of 200 and 25 mM, respectively. Absorption spectra were measured on a Varian Cary 4000 spectrophotometer. Concentration of the zinc porphyrin−DNA complex was set to ∼1 μM using $\varepsilon_{545} = 1.4 \times 10^4\ M^{-1}\ cm^{-1}$, unless otherwise stated. Steady-state fluorescence was measured on a Spex Fluorolog 3 spectrofluorimeter (JY Horiba) by exciting the samples at 543 nm. Circular dichroism (CD) spectra were recorded on a Chirascan Applied Photophysics spectropolarimeter at 20 °C in the absence of liposomes.

Linear dichroism (LD) spectra were recorded on a modified Jasco J-720 CD spectropolarimeter fitted with an Oxley prism to produce linearly polarized light. A Couette cell was used to induce shear flow orientation of the samples. Measurements were performed in 50% w/w sucrose of the same Tris-HCl buffer solution at a lipid and porphyrin−DNA complex concentration of 500 and 2.5 μM, respectively. The sucrose fulfils two roles: first, refractive index matching of the liposomes to the solution greatly reduces detection problems caused by polarized light scattering, and second, the increased viscosity provides for better alignment of the liposomes.[36] The background at zero shear rate was used as a baseline for the spectra taken at a shear gradient of 3100 $s^{-1}$. Isotropic absorption measurements were made on the same samples to calculate the $LD^r$ spectrum.

The binding constants of the porphyrin−DNA complexes to liposomes were determined by spectrophotometric titration. The titrations were performed by adding aliquots of a liposome stock solution to the porphyrin−DNA adduct solution. Corrections for the volume change were made in the subsequent analysis.

Fluorescence lifetimes were determined using time-correlated single photon counting. The samples were excited using a 405 nm pulsed laser diode (PicoQuant GMBA). The photons were collected by a thermoelectrically cooled microchannel plate photomultiplier tube (MCP-PMT R3809U-50; Hamamatsu) and fed into a multichannel analyzer with 4096 channels. A minimum of 10 000 counts were recorded in the top channel. The fluorescence decay curves were fitted to double-exponential expressions by the program FluoFit Pro v.4 (PicoQuant GMBA). The sample response was recorded through a 550 nm low pass filter to reject scattered light and monitored through a monochromator at 579 ± 16 nm.

The femtosecond setup has been described in detail elsewhere.[37] The samples were the bi-pe and tri-pe complexes in a liposome environment, kept in 2 mm cuvettes. For the electron transfer verification experiments, benzoquinone was added to the solution at concentrations corresponding to 50% quenching of the porphyrin steady-state emission. The optical densities of the samples were between 0.6 and 1.0 at the excitation wavelength 420 nm (*i.e.*, the Soret band peak). The probe and reference beams were, after passing the sample, focused on optical fibers connected to a spectrograph (Shamrock sr-303i, Andor) and detected at 1 kHz by a CCD camera (iXon $em^+$, Andor). One thousand scans were averaged for each delay time. The group velocity dispersion of the probe white light was fitted to a third-order polynomial and corrected by use of a MATLAB program. To make direct comparisons between signal amplitudes, the differential absorption signals were normalized to an optical density of 1 at the excitation wavelength.

*Acknowledgment.* This research is founded by King Abdullah University of Science and Technology, The Swedish Research Council (VR), The Swedish Energy Agency, and Knut and Alice Wallenbergs Foundation.

*Supporting Information Available:* Synthetic procedures and characterization, liposome binding isotherms, binding site and DNA area derivation, Stern−Volmer plots of fluorescence

quenching by benzoquinone, and transient absorption spectra of tri-pe with and without the presence of benzoquinone. This material is available free of charge *via* the Internet at http://pubs.acs.org.

## REFERENCES AND NOTES


1. Seeman, N. C. DNA in a Material World. *Nature* **2003**, *421*, 427–431.
2. Andersen, F. F.; Knudsen, B.; Oliveira, C. L. P.; Frohlich, R. F.; Kruger, D.; Bungert, J.; Agbandje-McKenna, M.; McKenna, R.; Juul, S.; Veigaard, C.; *et al.* Assembly and Structural Analysis of a Covalently Closed Nano-Scale DNA Cage. *Nucleic Acids Res.* **2008**, *36*, 1113–1119.
3. Erben, C. M.; Goodman, R. P.; Turberfield, A. J. A Self-Assembled DNA Bipyramid. *J. Am. Chem. Soc.* **2007**, *129*, 6992–6993.
4. Park, S. H.; Pistol, C.; Ahn, S. J.; Reif, J. H.; Lebeck, A. R.; Dwyer, C.; LaBean, T. H. Finite-Size, Fully Addressable DNA Tile Lattices Formed by Hierarchical Assembly Procedures. *Angew. Chem., Int. Ed.* **2006**, *45*, 735–739.
5. Tumpane, J.; Kumar, R.; Lundberg, E. P.; Sandin, P.; Gale, N.; Nandhakumar, I. S.; Albinsson, B.; Lincoln, P.; Wilhelmsson, L. M.; Brown, T.; *et al.* Triplex Addressability as a Basis for Functional DNA Nanostructures. *Nano Lett.* **2007**, *7*, 3832–3839.
6. Tumpane, J.; Sandin, P.; Kumar, R.; Powers, V. E. C.; Lundberg, E. P.; Gale, N.; Baglioni, P.; Lehn, J. M.; Albinsson, B.; Lincoln, P.; *et al.* Addressable High-Information-Density DNA Nanostructures. *Chem. Phys. Lett.* **2007**, *440*, 125–129.
7. Balaz, M.; Holmes, A. E.; Benedetti, M.; Proni, G.; Berova, N. Porphyrin Substituted Phosphoramidites: New Building Blocks for Porphyrin-Oligonucleotide Syntheses. *Bioorg. Med. Chem.* **2005**, *13*, 2413–2421.
8. Balaz, M.; Holmes, A. E.; Benedetti, M.; Rodriguez, P. C.; Berova, N.; Nakanishi, K.; Proni, G. Synthesis and Circular Dichroism of Tetraarylporphyrin-Oligonucleotide Conjugates. *J. Am. Chem. Soc.* **2005**, *127*, 4172–4173.
9. Balaz, M.; Li, B. C.; Steinkruger, J. D.; Ellestad, G. A.; Nakanishi, K.; Berova, N. Porphyrins Conjugated to DNA as Cd Reporters of the Salt-Induced B to Z-DNA Transition. *Org. Biomol. Chem.* **2006**, *4*, 1865–1867.
10. Balaz, M.; Steinkruger, J. D.; Ellestad, G. A.; Berova, N. 5′-Porphyrin−Oligonucleotide Conjugates: Neutral Porphyrin−DNA Interactions. *Org. Lett.* **2005**, *7*, 5613–5616.
11. Mestre, B.; Jakobs, A.; Pratviel, G.; Meunier, B. Structure/Nuclease Activity Relationships of DNA Cleavers Based on Cationic Metalloporphyrin−Oligonucleotide Conjugates. *Biochemistry* **1996**, *35*, 9140–9149.
12. Mammana, A.; Asakawa, T.; Bitsch-Jensen, K.; Wolfe, A.; Chaturantabut, S.; Otani, Y.; Li, X. X.; Li, Z. M.; Nakanishi, K.; Balaz, M.; *et al.* Synthesis and Characterization of Water-Soluble Free-Base, Zinc and Copper Porphyrin−Oligonucleotide Conjugates. *Bioorg. Med. Chem.* **2008**, *16*, 6544–6551.
13. Berlin, K.; Jain, R. K.; Simon, M. D.; Richert, C. A Porphyrin Embedded in DNA. *J. Org. Chem.* **1998**, *63*, 1527–1535.
14. Murashima, T.; Hayata, K.; Saiki, Y.; Matsui, J.; Miyoshi, D.; Yamada, T.; Miyazawa, T.; Sugimoto, N. Synthesis, Structure and Thermal Stability of Fully Hydrophobic Porphyrin−DNA Conjugates. *Tetrahedron Lett.* **2007**, *48*, 8514–8517.
15. Endo, M.; Fujitsuka, M.; Majima, T. Diastereochemically Controlled Porphyrin Dimer Formation on a DNA Duplex Scaffold. *J. Org. Chem.* **2008**, *73*, 1106–1112.
16. Endo, M.; Shiroyama, T.; Fujitsuka, M.; Majima, T. Four-Way-Branched DNA−Porphyrin Conjugates for Construction of Four Double-Helix-DNA Assembled Structures. *J. Org. Chem.* **2005**, *70*, 7468–7472.
17. Endo, M.; Fujitsuka, M.; Majima, T. Programmable Conformational Regulation of Porphyrin Dimers on Geometric Scaffold of Duplex DNA. *Tetrahedron* **2008**, *64*, 1839–1846.
18. Morales-Rojas, H.; Kool, E. T. A Porphyrin C-Nucleoside Incorporated into DNA. *Org. Lett.* **2002**, *4*, 4377–4380.
19. Nguyen, T.; Brewer, A.; Stulz, E. Duplex Stabilization and Energy Transfer in Zipper Porphyrin−DNA. *Angew. Chem., Int. Ed.* **2009**, *48*, 1974–1977.
20. Fendt, L. A.; Bouamaied, I.; Thoni, S.; Amiot, N.; Stulz, E. DNA as Supramolecular Scaffold for Porphyrin Arrays on the Nanorneter Scale. *J. Am. Chem. Soc.* **2007**, *129*, 15319–15329.
21. Bouamaied, I.; Nguyen, T.; Ruhl, T.; Stulz, E. Supramolecular Helical Porphyrin Arrays Using DNA as a Scaffold. *Org. Biomol. Chem.* **2008**, *6*, 3888–3891.
22. Börjesson, K.; Tumpane, J.; Ljungdahl, T.; Wilhelmsson, L. M.; Nordén, B.; Brown, T.; Mårtensson, J.; Albinsson, B. Membrane-Anchored DNA Assembly for Energy and Electron Transfer. *J. Am. Chem. Soc.* **2009**, *131*, 2831–2839.
23. Ljungdahl, T.; Pettersson, K.; Albinsson, B.; Mårtensson, J. Solvent and Base Dependence of Copper-Free Palladium-Catalyzed Cross-Couplings between Terminal Alkynes and Arylic Iodides: Development of Efficient Conditions for the Construction of Gold(III)/Free-Base Porphyrin Dimers. *J. Org. Chem.* **2006**, *71*, 1677–1687.
24. Nordén, B.; Kubista, M.; Kurucsev, T. Linear Dichroism Spectroscopy of Nucleic-Acids. *Q. Rev. Biophys.* **1992**, *25*, 51–170.
25. Ardhammar, M.; Mikati, N.; Nordén, B. Chromophore Orientation in Liposome Membranes Probed with Flow Dichroism. *J. Am. Chem. Soc.* **1998**, *120*, 9957–9958.
26. Svensson, F. R.; Lincoln, P.; Nordén, B.; Esbjörner, E. K. Retinoid Chromophores as Probes of Membrane Lipid Order. *J. Phys. Chem. B* **2007**, *111*, 10839–10848.
27. Gouterman, M. Spectra of Porphyrins. *J. Mol. Spectrosc.* **1961**, *6*, 138–163.
28. Kilså, K.; Kajanus, J.; Macpherson, A. N.; Mårtensson, J.; Albinsson, B. Bridge-Dependent Electron Transfer in Porphyrin-Based Donor-Bridge-Acceptor Systems. *J. Am. Chem. Soc.* **2001**, *123*, 3069–3080.
29. Pfeiffer, I.; Höök, F. Bivalent Cholesterol-Based Coupling of Oligonucletides to Lipid Membrane Assemblies. *J. Am. Chem. Soc.* **2004**, *126*, 10224–10225.
30. Kilså, K.; Macpherson, A. N.; Gillbro, T.; Mårtensson, J.; Albinsson, B. Control of Electron Transfer in Supramolecular Systems. *Spectrochim. Acta, Part A* **2001**, *57*, 2213–2227.
31. East, J. M.; Lee, A. G. Lipid Selectivity of the Calcium and Magnesium-Ion Dependent Adenosine-Triphosphatase, Studied with Fluorescence Quenching by a Brominated Phospholipid. *Biochemistry* **1982**, *21*, 4144–4151.
32. Kaneko, M.; Tsuchida, E.; Imai, Y. Incorporation and Distribution of Benzoquinone into Liposomes Containing Amphilic Zinc(II) Porphyrin as Studied by the Quenching of the Excited-State. *J. Chem. Soc., Faraday Trans.* **1991**, *87*, 83–86.
33. Fajer, J.; Borg, D. C.; Forman, A.; Dolphin, D.; Felton, R. H. π-Cation Radicals and Dications of Metalloporphyrins. *J. Am. Chem. Soc.* **1970**, *92*, 3451–3459.
34. Chosrowjan, H.; Tanigichi, S.; Okada, T.; Takagi, S.; Arai, T.; Tokumaru, K. Electron-Transfer Quenching of S-2 State Fluorescence of Zn-Tetraphenylporphrin. *Chem. Phys. Lett.* **1995**, *242*, 644–649.
35. Imahori, H.; Hagiwara, K.; Aoki, M.; Akiyama, T.; Taniguchi, S.; Okada, T.; Shirakawa, M.; Sakata, Y. Linkage and Solvent Dependence of Photoinduced Electron Transfer in Zincporphyrin-C-60 Dyads. *J. Am. Chem. Soc.* **1996**, *118*, 11771–11782.
36. Ardhammar, M.; Lincoln, P.; Nordén, B. Invisible Liposomes: Refractive Index Matching with Sucrose Enables Flow Dichroism Assessment of Peptide Orientation in Lipid Vesicle Membrane. *Proc. Natl. Acad. Sci. U.S.A.* **2002**, *99*, 15313–15317.
37. Pettersson, K.; Wiberg, J.; Ljungdahl, T.; Mårtensson, J.; Albinsson, B. Interplay between Barrier Width and Height in Electron Tunneling: Photoinduced Electron Transfer in Porphyrin-Based Donor-Bridge-Acceptor Systems. *J. Phys. Chem. A* **2006**, *110*, 319–326.